Available online at www.sciencedirect.com
SCIENCE DIRECT®
Physics Letters A 324 (2004) 71–81
PHYSICS LETTERS A
www.elsevier.com/locate/pla

Magnetic and superconducting behaviours of doped and undoped double perovskite Ba_2PrRuO_6

S.M. Rao [a], M.K. Wu [a,b], J.K. Srivastava [c,*], B.H. Mok [b], C.Y. Lu [b], Y.C. Liao [b], Y.Y. Hsu [a], Y.S. Hsiue [a], Y.Y. Chen [a], S. Neeleshwar [a], S. Tsai [a], J.C. Ho [d], H.-L. Liu [e]

[a] *Institute of Physics, Academia Sinica, Nankang, Taipei 115, Taiwan, ROC*
[b] *Department of Physics and Materials Science Center, National Tsing Hua University, Hsinchu, Taiwan, ROC*
[c] *Tata Institute of Fundamental Research, Mumbai 400005, India*
[d] *Department of Physics, Wichita State University, Wichita, KS 67260-0032, USA*
[e] *Department of Physics, National Taiwan Normal University, Taipei 116, Taiwan, ROC*

Received 20 October 2003; accepted 11 February 2004

Communicated by J. Flouquet

Abstract

Our detailed measurements show the undoped double perovskite $Ba_2^{2+}Pr^{3+}Ru^{5+}O_6^{2-}$ to be a nonmetallic (insulating) spin glass (SG) and the ∼ 5–10% Cu-doped (i.e., Cu-concentration/(Cu + Ru-concentration) ∼ 5–10%) system to be a spin glass superconductor (SGSC), though the critical temperature, T_c, (∼ 8–11 K) and the superconducting volume fraction, f_{sc}, (∼ 1–4%) are small. This smallness is presumably due to the presence of a large number of pair breaking spins and small carrier concentration in the lattice. Results and their implications are discussed.

PACS: 74.25.Ha; 74.72.-h; 74.72.Yg; 75.50.Lk

Keywords: Double perovskite; Cuproruthenate; High-T_c superconductivity; Magnetic superconductor; Frustration; Spin glass

1. Introduction

In recent years, after the discovery of superconductivity in Sr_2RuO_4 [1], research workers have started examining the magnetism and conductivity of Ru-based oxides [2–9]. Ba_2PrRuO_6 (BaPr2116 for brevity) belongs to the large family of double perovskites being investigated by several groups [10–16]. Izumiyama et al. [10] studied polycrystalline samples of BaPr2116 prepared by high temperature sintering of stoichiometric powders. Their study reports for the system an antiferromagnetic transition temperature (T_N) of 117 K, above which, as shown by neutron diffraction measurements, no long range magnetic ordering exists in the lattice. Wu and coworkers [2–4] investigated polycrystalline samples of a similar family of double perovskites, namely $Ba_2YRu_{1-x}Cu_xO_6$ (BaYCu2116) and $Sr_2YRu_{1-x}Cu_xO_6$ (SrYCu2116)

* Corresponding author.
E-mail address: jks@tifr.res.in (J.K. Srivastava).

0375-9601/$ – see front matter
doi:10.1016/j.physleta.2004.02.029

and reported coexistence of superconductivity and magnetism for $x = 0.05$ to 0.2. We have grown the single crystals of undoped and Cu-doped Ba_2PrRuO_6 from high temperature solutions. The magnetic and superconducting properties of these grown $Ba_2PrRu_{1-x}Cu_xO_\delta$ (BaPrCu2116) single crystals ($x = 0$–0.2, $\delta = 6$ or ~ 6) are presented in this Letter alongwith the results of the supporting SEM (scanning electron microscope), EDX (energy dispersive X-ray), Raman, XRD (X-ray diffraction) and specific heat investigations. The study brings out the spin glass (SG) and spin glass superconductor (SGSC) nature of the system for different x values.

2. Experimental

The undoped and Cu-doped BaPr2116 powders were prepared by the solid state reaction of a stoichiometric mixture of $BaCO_3$, Pr_6O_{11}, Ru and CuO constituent materials. These constituents (in powder form) were made to react in air at 1050 °C for three times to ensure completion of the reaction which was confirmed by powder X-ray diffraction analysis. Crystals were grown from high temperature solutions. The solvent consisted of a 60:40 mixture of $PbO:PbF_2$ (flux). The solute, BaPr2116 powder (undoped or Cu-doped), with a weight of $\sim$ 10–20% of $PbO:PbF_2$ mixture weight, was added to the solvent. The solute and solvent, $\sim$ 3–6 gram, were thoroughly mixed and packed in a platinum crucible covered with a platinum lid. The crucible was placed in the crystal growing furnace which could be heated by programmed heating to melt the solvent–solute mixture, soak and grow crystals by slow cooling. The slow cooling was done from several temperatures (called growth temperature (GT)) in the range 1125 to 1200 °C. As is explained later, the results presented in this Letter are for the crystals grown at 1180 °C (i.e., GT = 1180 °C). In their case, the solute–solvent mixture was heated to 1180 °C, soaked for 6–8 hours to homogenise and then cooled at the rate of 0.2 to 0.5 °C per hour to 1165 °C. From there the crucible was cooled at a faster rate (50–150 °C per hour) to room temperature. Finally the crucible was removed from the furnace, excess flux was drained off and crystals were taken out. During the crystal growth (i.e., during 1180–1165 °C cooling period) the crucible was rotated clockwise and anticlockwise at 20–25 rpm with a hold time, between reversals, of 30–40 seconds. Typical growth programme took nearly 3–5 days. The magnetic and superconducting properties of the grown crystals were investigated using SQUID magnetometer. Due to the small size of the crystals (average upper face diameter 1–2 mm, thickness 0.2–0.5 mm) we could not carry out the resistivity measurements.

3. Results and discussion

Fig. 1(a) shows a typical as grown crystal. The morphology of the crystals varied from elongated hexagonal plates to triangular or hexagonal plates stacked together. The superconducting critical temperature, T_c, and superconducting volume fraction, f_{sc}, obtained from the SQUID data shown below [3], were found to depend on x and GT. The recorded data also showed that the superconductivity existed in the studied system ($Ba_2PrRu_{1-x}Cu_xO_\delta$) only for $0.05 \leqslant x \leqslant 0.1$. In this range for the 1180 °C-grown sample (GT = 1180 °C), the T_c, f_{sc} increased from 8 K, 1% for $x = 0.05$ to 11 K, 4% for $x = 0.075$ and then decreased to 8 K, 2.5% for $x = 0.1$ when H (external magnetic field) = 20 Oe. Increasing GT above 1180 °C did not change T_c or f_{sc}. However, when GT was decreased, T_c and f_{sc} decreased. For the 1130 °C-grown sample (GT = 1130 °C, slow cooling range = 1130–1110 °C (as compared to 1180–1165 °C range of 1180 °C-grown sample)), $T_c = 9$ K and $f_{sc} = 1.5\%$ when $x = 0.075$, $H = 20$ Oe. When these grown samples were subjected to post growth annealing, T_c and f_{sc} changed again. For example, when 1130 °C-grown $x = 0.075$ sample (crystal) was annealed at 1200 °C in 50:50 O:Ar flowing gas atmosphere, the annealed crystal showed $T_c = 11$ K and $f_{sc} = 1.5\%$ for $H =$ 20 Oe. When the as grown sample was annealed in pure oxygen (flowing) atmosphere, superconductivity was not observed. In this Letter, all the given results (Figs. 1, 3–6) belong to the as grown crystals ($x = 0, 0.075$) with GT = 1180 °C except those of Fig. 2 ($x = 0.075$) which have been given only to show the effects of GT and post growth annealing on sample properties. It is clearly seen there that T_c, obtained by the temperatures at which the curves a, a′ start taking negative values, gets increased on post growth O:Ar annealing (i.e., $(T_c)_{a'} > (T_c)_a$).

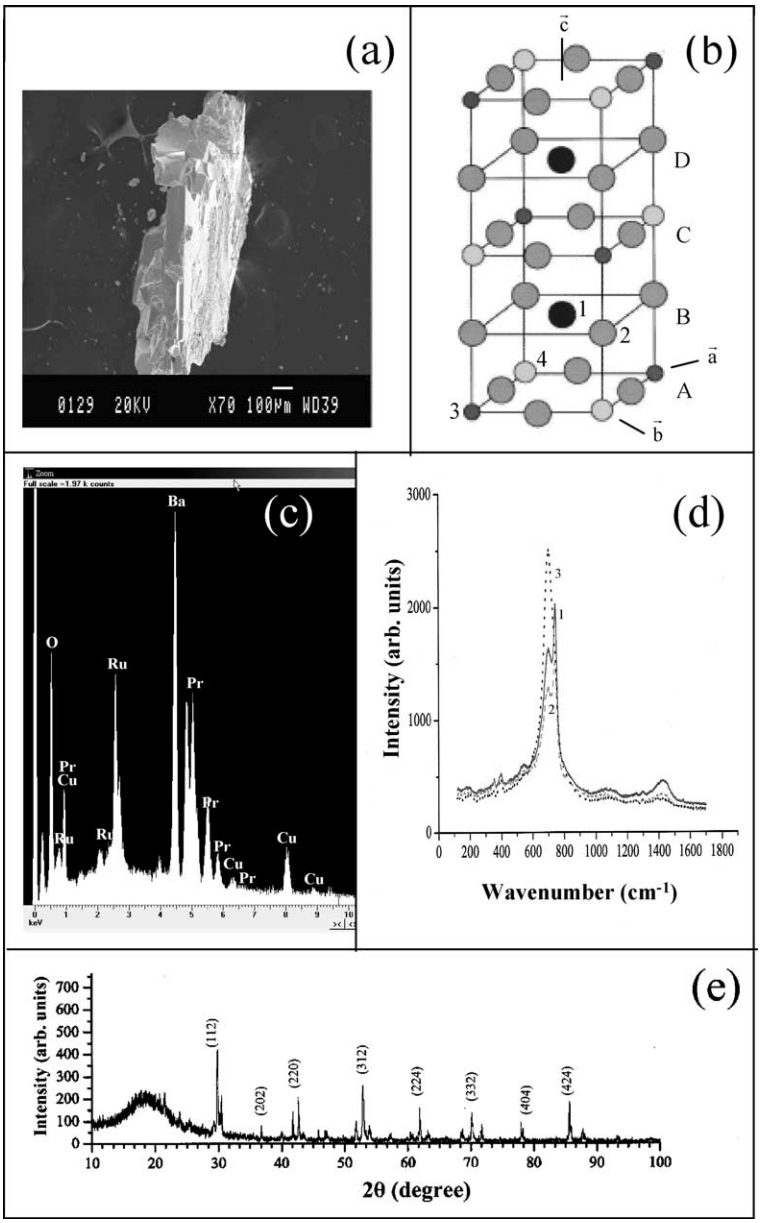

Fig. 1. (a) A typical crystal habit (SEM micrograph). The crystal shown is an as grown $Ba_2PrRu_{1-x}Cu_xO_\delta$ crystal ($x = 0.075$, GT (growth temperature) = 1180 °C). (b) Crystal structure of Ba_2PrRuO_6; the ion positions are 1 = Ba, 2 = O, 3 = Ru (predominantly), 4 = Pr (predominantly). A, B, C, D, are the various planes and $\vec{a}$, $\vec{b}$, $\vec{c}$ the crystallographic axes. (c) EDX spectrum of as grown, GT = 1180 °C $Ba_2PrRu_{1-x}Cu_xO_\delta$ ($x = 0.075$) system. For the GT = 1130 °C sample, the observed Cu peaks are of smaller intensity. (d) Raman spectrum (intensity vs. Raman shift) recorded for the as grown, GT = 1180 °C $Ba_2PrRu_{1-x}Cu_xO_\delta$ system ($x = 0$ (curve 1), 0.075 (curve 2) and 0.1 (curve 3)). (e) Powder X-ray diffraction pattern recorded for powdered as grown, GT = 1180 °C $Ba_2PrRu_{1-x}Cu_xO_\delta$ ($x = 0.075$) single crystal.

Fig. 1(a), (c)–(e) give results obtained for the 1180 °C-grown $x = 0.075$ sample and Fig. 1(b) shows the BaPr2116 crystal structure. The presence of Cu peaks in Fig. 1(c) confirms the incorporation of Cu in the doped lattice. These peaks are of small intensity in the 1130 °C-grown crystal, indicating doped

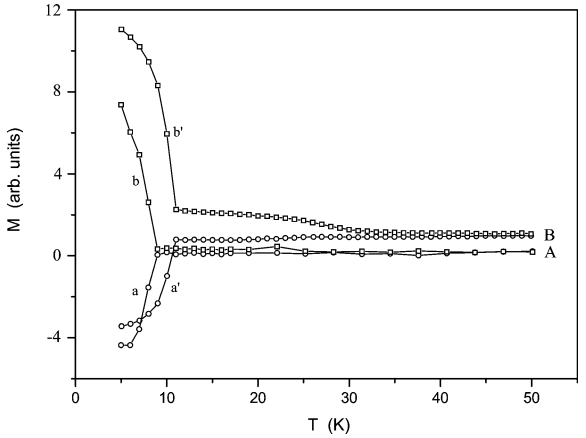

Fig. 2. Magnetisation (M) vs. temperature (T) variation for (A) as grown $x = 0.075$, GT = 1130 °C $Ba_2PrRu_{1-x}Cu_xO_\delta$ sample (curve a, b) and (B) the same as grown sample after that has been annealed at 1200 °C for 12 hours in 50:50 O:Ar flowing gas atmosphere (curve a′, b′). Curve a, a′ are for the zero field cooled (ZFC) case and curve b, b′ for the field cooled (FC) case; H (external magnetic field) = 20 Oe. For recording the ZFC–FC curve, sample has been first cooled in zero field to lowest T and H applied there. With H present, M vs. T has been recorded upto 300 K (room temperature) (ZFC curve). After that the sample has been cooled back in the same H to lowest T and M vs. T recorded again with T increasing and H present (FC curve).

$x < 0.075$ there, which explains the reason for smaller T_c and f_{sc} in those crystals. Preliminary Raman investigations too confirm the incorporation of Cu in the doped crystal by showing a change in the spectrum with x (Fig. 1(d)). All the samples were investigated by X-ray diffraction and Fig. 1(e) gives a typical XRD pattern obtained for $x = 0.075$ sample. The peak positions shift, though by small amount, to lower (higher) θ values with increasing (decreasing) x. Analysis of these patterns yields lattice parameters (± 0.005 Å, $\pm 0.04°$) for $x = 0$ as $a = 5.999$, $b = 5.982$, $c = 8.469$ and $\beta = 89.98$, showing monoclinic structure in agreement with the published data [10], and for $x = 0.075$ as $a = 6.003$, $b = 5.984$, $c = 8.480$ and $\beta = 90.05$.

Fig. 3(A) shows the M (magnetisation)–T (temperature) curve recorded for $x = 0$ sample; curve a is for ZFC (zero field cooled) sample, curve b for FC (field cooled) sample and $H = 50$ Oe. The nature of the ZFC curve (curve a) is similar to that observed by Izumiyama et al. [10] for their powder sample. The broad peak seen by us around 100 K has been observed by them also. However, they have not extended their FC measurements below 100 K, whereas we find the presence of magnetic irreversibility, M_{irr}, (branching of ZFC and FC magnetisation (M(ZFC), M(FC)) curves) below ~ 80 K indicating that the $x = 0$ sample is probably a reentrant SG [17,18]. The peak observed by us at ~ 25 K (curve a) has been seen by Izumiyama et al. also as a broad anomaly but they have not commented about it. We also find for the $x = 0$ sample (Fig. 4(A)) a nonlinear M–H variation even above ~ 100 K where the system is paramagnetic according to Izumiyama et al. [10] and therefore a linear M–H dependence is expected. The nonlinearity persists upto 300 K, our highest measurement temperature, and can be seen clearly by M/H vs. H plot since for a linear M–H variation, M/H will not change with H. This nonlinearity indicates the presence of magnetic clusters in the otherwise paramagnetic system. The fact that no magnetic hysteresis is seen by us above ~ 100 K is consistent with the conclusion of Izumiyama et al. [10] about the absence of any long range magnetic ordering in BaPr2116 above 117 K. Such a behaviour (presence of clusters and no long range ordering above a certain temperature) has been seen in other SG systems also [17,19]. In a reentrant SG system there are four transition temperatures, namely T_{CF}, T_C or T_N, T_{M1} and T_{M2}; normally $T_{CF} > T_C$, $T_N > T_{M1} > T_{M2}$ (but near tricritical point, the T_C, T_{M1} may be quite close) [17,18]. As one cools the lattice, at T_{CF} magnetic clusters are formed in the material's otherwise paramagnetic state. The magnetic ordering inside clusters can be ferro-, ferri- or antiferromagnetic. Assigning a spin $\vec{S}_{cl}$ to a cluster (lattice/sublattice), at T_C or T_N the z-component of $\vec{S}_{cl}$, $(\vec{S}_{cl})_z$, of all clusters get magnetically ordered and the x, y components, $(\vec{S}_{cl})_x$, $(\vec{S}_{cl})_y$, average out to zero; T_N is Néel temperature, T_C is ferro- or ferrimagnetic Curie temperature. On further cooling, at T_{M1} $(\vec{S}_{cl})_z$ remain magnetically ordered but $(\vec{S}_{cl})_x$, $(\vec{S}_{cl})_y$ freeze in SG configuration (random direction pointing on the average). Finally at T_{M2}, all the three components, $(\vec{S}_{cl})_z$, $(\vec{S}_{cl})_x$, $(\vec{S}_{cl})_y$, get randomly frozen in SG configuration. From the Figs. 3(A), 4(A) discussions given above we conclude that for $x = 0$ sample, $T_{CF} > 300$ K, $T_C \sim 100$ K (we call it T_C since we find the presence of magnetic hysteresis below ~ 100 K indicating a ferrimagnetic ordering), $T_{M1} \sim 80$ K (below which M_{irr} appears) and $T_{M2} \sim 25$ K (below which M_{irr} becomes strong and at

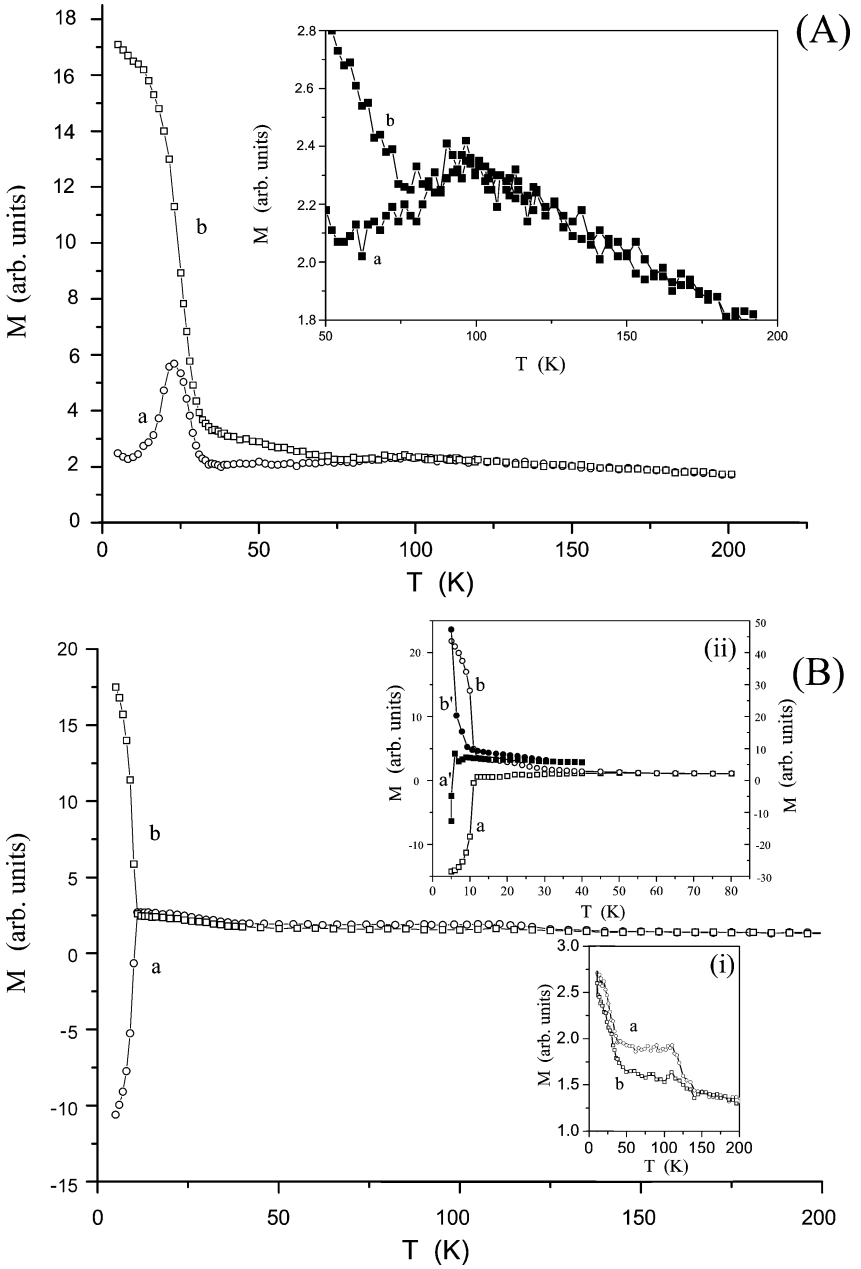

Fig. 3. Temperature (T) dependence of magnetisation (M) for as grown, GT = 1180 °C $Ba_2PrRu_{1-x}Cu_xO_\delta$; curves a, a′ are for ZFC case and b, b′ for FC case. (A) $x = 0$, H (external field) = 50 Oe. Inset shows enlarged view showing ∼ 100 K transition. (B) $x = 0.075$, $H = 20$ Oe. Inset (i) shows enlarged view of a main figure portion ($H = 20$ Oe) showing ∼ 100 K transition and inset (ii) shows M–T curves recorded for $H = 25$ Oe (curve a, b) and 50 Oe (curve a′, b′). In inset (ii), the left (right) hand side y-axis scale is for open (filled) data points.

which ZFC curve has a peak). The above conclusion is supported by the specific heat measurements ([10], Fig. 5 (curve a)) also. Izumiyama et al. [10] measured specific heat for $x = 0$ powder sample in the 2–300 K range and apart from ∼ 100 K peak (Λ-type anomaly) found no other anomaly in the specific heat (C)

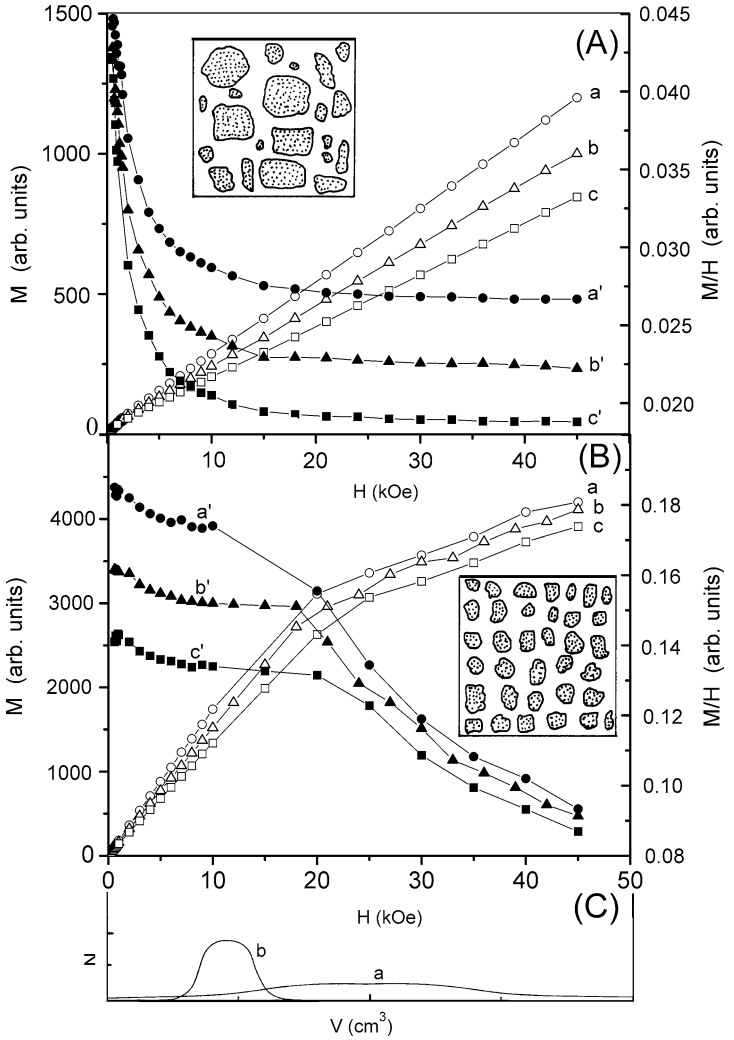

Fig. 4. M (magnetisation), M/H vs. H (external magnetic field) for as grown, GT = 1180 °C $Ba_2PrRu_{1-x}Cu_xO_\delta$ system; $x = 0$ (A), 0.075 (B). Temperature $T = 150$ K (a, a′), 200 K (b, b′) and 250 K (c, c′). Left (right) hand side y-axis scale is for open (filled) data points. Insets show the probable cluster size distributions, for $x = 0$ (inset (A)) and $x = 0.075$ (inset (B)), inferred from M–H variations. (C) If the actual histogram of a cluster size distribution is replaced by a smooth continuous curve, then the distributions can be represented approximately by curve a ($x = 0$) and curve b ($x = 0.075$); N is number, V is volume of clusters (schematic representation).

vs. T curve. This supports the SG nature of T_{M1}, T_{M2} transitions since specific heat is known not to show any anomaly at SG (random freezing) transitions [18,20]. Our single crystal specific heat measurement results are same as those of Izumiyama et al. [10]. In Fig. 5 curve a ($x = 0$), we have plotted only the low temperature ($T < 45$ K) part of the specific heat curve to show that when plotted as C/T vs. T^2, the data show a sharp increase in the C/T value at very low temperatures ($\lesssim 2.5$ K). Such an increase shows the presence of magnetic clusters in the system [21]. We find that this SG nature, with magnetic clusters, is present in all the samples studied by us for $0 \leqslant x \leqslant 0.2$. In addition, the samples with $x = 0.05$–0.1 show the presence of superconductivity also. As an example, we discuss below the results of the $x = 0.075$ sample.

Fig. 3(B) shows the M–T curve for $x = 0.075$ sample (ZFC curve (curve a), FC curve (curve b), $H =$

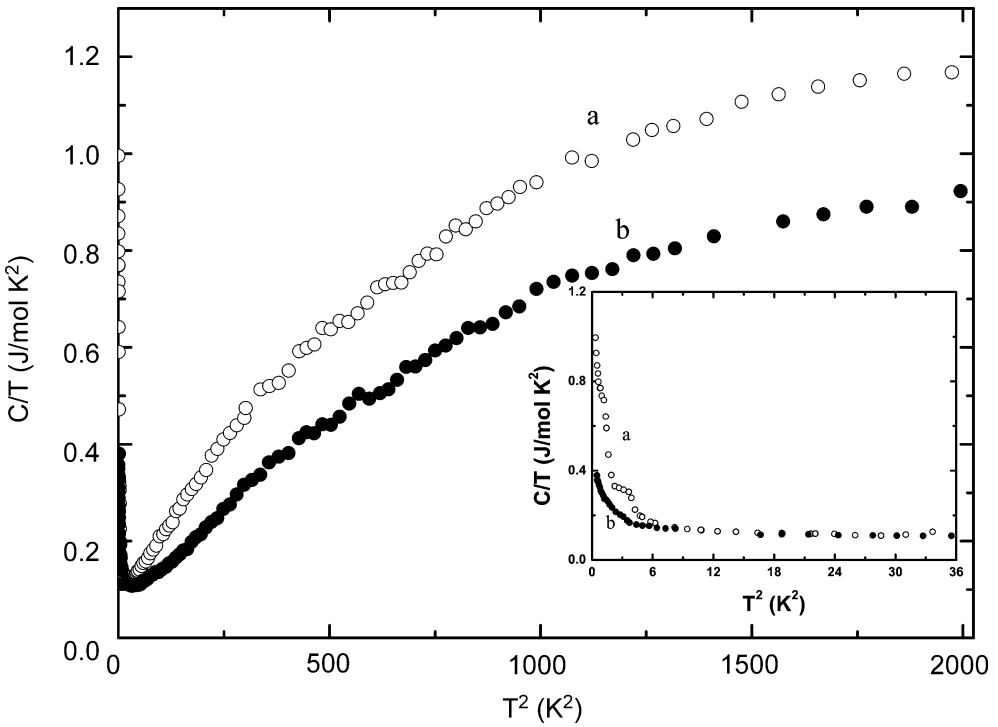

Fig. 5. Temperature (T) dependence of the specific heat (C) plotted as C/T vs. T^2 for the as grown, GT = 1180 °C $Ba_2PrRu_{1-x}Cu_xO_\delta$; $x = 0$ (curve a), $x = 0.075$ (curve b), H (external field) = 0. Inset shows expanded view of curve a, b low temperature ($T < 6$ K) portion.

20 Oe). A careful examination shows that the broad ~ 100 K-peak is still there; this is seen more clearly in inset (i). In addition, the M_{irr} temperature has shifted to below 50 K. Increasing H to 25 Oe shows this clearly (inset (ii), curve a (ZFC case), curve b (FC case), M_{irr} seen below 45 K). Like the case of $x = 0$ sample, for $x = 0.075$ sample also the M–H variation shows the presence of clusters above ~ 100 K (Fig. 4(B)) and the specific heat measurement indicates this presence upto the lowest measurement temperature (Fig. 5 curve b). The long range magnetic ordering and SG freezing via frustrated intercluster interaction have been concluded to be present in some other systems also [22]. From our above described measurements we conclude that for the $x = 0.075$ sample, $T_{CF} > 300$ K, $T_C \sim 100$ K, $T_{M1} \sim 45$ K and $T_{M2} \sim 11$ K. However, in this case, T_{M2} coincides with the superconducting transition temperature T_c since strong M_{irr} start (curve a (M(ZFC)), curve b (M(FC)) separation) and superconducting transition (beginning of $-M$(ZFC) values (curve a)) occur together (Fig. 3(B)). Increasing H to 50 Oe (Fig. 3(B) inset (ii), curve a′ (ZFC case), curve b′ (FC case)) separates T_c and T_{M2}, decreasing them both, respectively, to 6 and 9.5 K. This is consistent with the known T_c, T_{M2} vs. H behaviour [4,18,23]. Thus the $x = 0.075$ system can be called a spin glass superconductor (SGSC), though the superconductivity is weak for reasons discussed later. This SGSC nature of $x = 0.075$ sample is confirmed by the magnetic hysteresis measurement also (Fig. 6). In Fig. 6, a large $-H$ shift is seen in the hysteresis curve centre on field cooling (curve a (ZFC), curve b (FC)). This is known to be a SG system's property [18,19]. In addition, Fig. 6 inset, showing the initial part of the ZFC hysteresis curve's first branch (enlarged view), clearly shows the superconducting diamagnetic response of the system yielding H_{c1} (lower critical field) ~ 8 Oe and H_{c2} (upper critical field) ~ 60 Oe. These H_{c1}, H_{c2} values are approximate since the observed curve is a sum of superconducting state (supercurrent plus trapped flux contribution) and SG state (Pr, Ru frozen moments' contribution) curves. Nevertheless, they indicate the probable smallness of H_{c1}, H_{c2}. Small H_{c1},

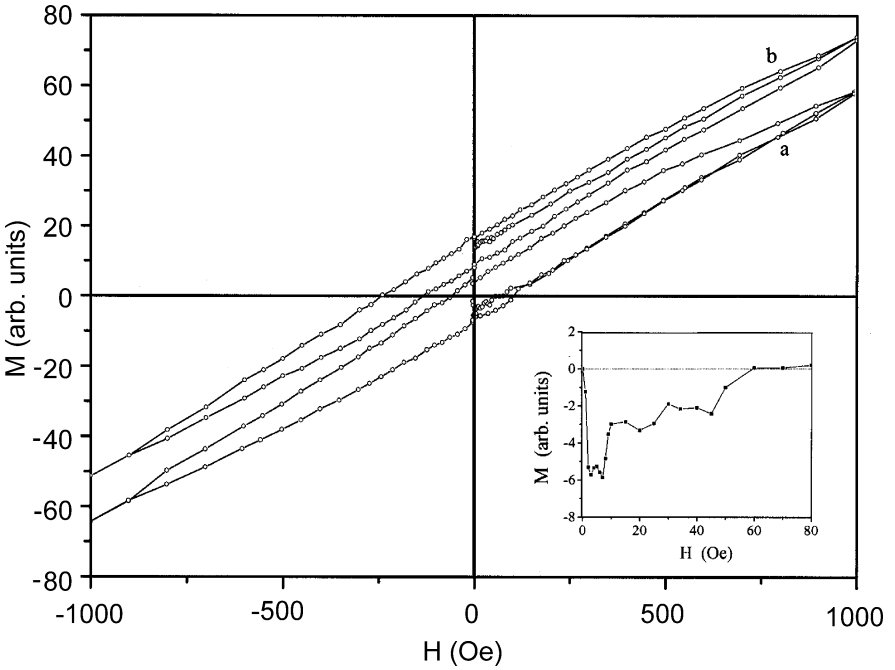

Fig. 6. Magnetic hysteresis curve recorded for the as grown, GT = 1180 °C $Ba_2PrRu_{1-x}Cu_xO_\delta$ ($x = 0.075$) system at $T = 5$ K for zero field cooled (ZFC) case (curve a) and field cooled (FC) case (curve b); M is magnetisation, H is external magnetic field. The curve b has been recorded after cooling the sample in $H = 20$ Oe from 300 K (room temperature). Inset shows an enlarged view of the low field portion of ZFC curve's (curve a's) first branch (starting branch situated between 0 and +1 kOe H values).

H_{c2} values show the weak superconducting nature of the $x = 0.075$ sample. The specific heat data (Fig. 5) too reveal this nature by not showing any anomaly at T_c. Even in normal (non-Ru) cuprates, where f_{sc} is large ($\sim$ 30–70%), the T_c specific heat anomaly is either very small or absent [24]. Thus it is not surprising that specific heat anomaly is not seen at T_c ($\sim$ 11 K) in $x = 0.075$ sample, where f_{sc} is only $\sim$ 4%. Our statement looks valid since, as discussed later, in all probability our crystals are pure and homogeneous.

In Fig. 6 the fact that just a 20 Oe field cooling gives a large $-H$ shift to the ZFC hysteresis loop centre indicates the involvement of clusters, as clusters will get affected even by a small field. Fig. 4 insets schematically show the expected, from M, M/H vs. H variations, cluster size distributions for $x = 0$ and 0.075 samples. In $x = 0$ case (Fig. 4(A)), M–H variation is nonlinear for small H and becomes more and more linear at higher H. This shows, for $x = 0$ system, the presence of large size clusters with a broad cluster size distribution (Fig. 4(A) inset, Fig. 4(C) curve a), so that even at higher H enough small size unaligned clusters are present and the M–H curve has no saturation tendency. Opposite is the M–H behaviour in Fig. 4(B) and so for $x = 0.075$ sample, clusters are smaller in size with narrower cluster size distribution (Fig. 4(B) inset, Fig. 4(C) curve b). The reason for the occurrence of such distributions (Fig. 4(A), (B) insets, Fig. 4(C)) is discussed later.

The origin of the SG behaviour of $x = 0$ sample and SGSC nature of $x = 0.075$ sample can be understood as follows. For the $x = 0$ case (Fig. 1(b)), if all the Ru ions (Ru^{5+}, $4d^3$) occupied unit cell site 3 and all the Pr ions (Pr^{3+}, $4f^2$) unit cell site 4 in the lattice, an uniform distribution of cations would have existed resulting in an uniform antiferromagnetic ordering as was thought to be the case by Izumiyama et al. [10]. However, if just $\sim$ 10–15% of Ru and Pr ions have got randomly substituted at each other's site, which is possible [18,19], magnetic frustration would occur in the lattice, owing to a difference in Ru^{5+} ($2\mu_B$), Pr^{3+} ($2.2\mu_B$) moments [10] and in $J_{Ru–Ru}$, $J_{Ru–Pr}$, $J_{Pr–Pr}$ exchange coupling strengths, making the system a reentrant SG [18,25]. At T_C the ordering will be

ferrimagnetic owing to the presence of antiparallely aligned unequal Ru, Pr moments.

The $x = 0$ system ($Ba_2^{2+}Pr^{3+}Ru^{5+}O_6^{2-}$) is an insulator. When Cu is introduced in this system, as in $x = 0.075$ sample, it presumably goes to the Ru site (ionic size effect) and the system becomes $Ba_2PrRu_{1-x}Cu_xO_\delta$ [4]. As in cuprates, Cu goes in the lattice in both Cu^{2+} and Cu^{3+} charge states and to maintain the charge neutrality, Ru^{4+} is created alongwith Ru^{5+} [8,9]. The $x \neq 0$ system becomes metallic presumably due to the $Cu^{2+} \rightleftarrows Cu^{3+}$ charge fluctuation presence as in cuprates [9,26]. Whether $Ru^{4+} \rightleftarrows Ru^{5+}$ charge fluctuation also exists cannot be said in the absence of detailed band structure calculations. However, presence of several ions with different magnetic moments (Cu^{2+}, Cu^{3+}, Ru^{4+}, Ru^{5+}, Pr^{3+}), whether in high or low spin states [8,9], gives rise to additional frustration in the lattice. This makes the average cluster sizes and cluster size distributions for the $x = 0$ and 0.075 systems different (Fig. 4). More explicitly, for the $x \neq 0$ case (Fig. 4(B)) the Pr–Ru–O layer area (Fig. 1(b)) gets divided into several short range ordered parts due to the presence of a large number of frustrating ions (i.e., randomly distributed Cu^{2+}, Cu^{3+}, Ru^{4+}, Ru^{5+}, Pr^{3+} ions which, even if in small numbers, break the long range uniform magnetic ordering [18]). Thus the clusters created are larger in number, smaller in size and narrower in cluster size distribution (Fig. 4). As with the magnetic ordering [10], a plane–plane interaction (like A–C coupling via B (Fig. 1(b))) can make the clusters three-dimensional in nature. Also, the presence of several antiparallely aligned dissimilar ions (Pr^{3+}, Ru^{4+}, Ru^{5+}) produces larger moment for the $x \neq 0$ case (Fig. 4). Several other observed results can also be understood in the same way. For instance, a change in annealing atmosphere (air, O : Ar, O) or GT or x changes Cu^{3+}/Cu^{2+} ratio in the system and affects T_c, f_{sc} as in cuprates [18]. Similarly, the positive value of M(FC), in the temperature range where M(ZFC) is negative (Figs. 2, 3), is a result of H being present during cooling in FC case. Due to this the moments get aligned/tilted along $\vec{H}$ during cooling giving large $+M$(FC). In cuprates, in the Cu–O plane where superconductivity resides, only Cu^{2+} moments are present which are presumably RVB (resonating valence bond) singlet paired [18]. In the $x \neq 0$ (BaPrCu2116) system, in the Pr–Ru–O layer (Fig. 1(b) (which now contains Cu also)) the Cu^{2+} spins are presumably still RVB singlet paired (due to the same reasons which existed in cuprates ($S = 1/2$, presence of frustration, layer structure, strong hybridisation)), but Pr^{3+}, Ru^{4+}, Ru^{5+} spins have no singlet pairing and so get affected by $\vec{H}$ and also cause Cooper pair breaking. This explains the small T_c, f_{sc} for $x \neq 0$ system. A small carrier concentration ($0.05 \leqslant x \leqslant 0.1$) is another reason for small T_c, f_{sc} ($x \neq 0$).

4. Conclusion

In conclusion, the BaPrCu2116 system is a SG for $0 \leqslant x \leqslant 0.2$ and a SGSC for $0.05 \leqslant x \leqslant 0.1$. This conclusion is consistent with the recent study results of $RuSr_2Gd_{1.5}Ce_{0.5}Cu_2O_{10-\delta}$ system [6] where SG nature, and clusters, have been found to coexist with superconductivity ($T_{CF} > 170$ K, $T_C \sim 100$ K, $T_{M1} \sim 68$ K, $T_{M2} \sim 45$ K, $T_c \sim 40$ K). It is also consistent with our recent SrYCu2116 results as well as with the paired cluster explanation of cuprate superconductivity which assumes the presence of SG interactions and clusters in cuprate superconductors [18]. Actually a closer examination of $RuSr_2GdCu_2O_8$ data [5] too shows some possibility of its being a SGSC ($T_{CF} \sim 200$ K, $T_C \sim 133$ K, $T_{M1} \sim T_C$, $T_{M2} \sim 20$ K, $T_c \sim 16$ K), though more work is needed to confirm this. It may be noted that in normal (non-Ru) cuprates where diamagnetism is very large and Cu^{2+} spins are presumably RVB singlet paired, it is difficult to detect the SG transition temperatures [18]. It may be further noted that the study of ruthenate superconductivity started with the idea of finding an alternate high-T_c system without Cu–O planes [1–4]. On the basis of our present work, the work on other ruthenocuprates mentioned here and the guidelines of paired cluster model [18], we find that a high-T_c ruthenium perovskite superconductor can be synthesised if the system has (i) a diamagnetic ion (like Y^{3+}) in place of magnetic Pr^{3+} ion, (ii) appreciable low symmetry (orthorhombic/monoclinic/triclinic) distortion so that Ru^{4+}, Ru^{5+} ions are in low crystal symmetry low spin state ($S = 0$ for Ru^{4+}, $S = 1/2$ for Ru^{5+}) and (iii) strong Ru–O hybridisation. This will create a situation (for Ru) similar to what is present (for Cu) in a cuprate Cu–O plane, namely the presence of (i) $Ru^{4+} \rightleftarrows Ru^{5+}$ charge fluctuation, (ii) magnetic frustration and clus-

ters, and (iii) RVB singlet coupling of two Ru^{5+} spins. It is hoped that this finding will start some new activity in the field.

At this point it may be worthwhile to mention that the absence of specific heat anomaly at the transition temperatures T_{M1}, T_{M2} and T_c can perhaps also be explained by assuming a sample inhomogeneity. However, our EDX measurements carried out on different portions of a crystal have yielded same EDX spectrum from these portions indicating crystals' compositional homogeneity. Also our T_c transitions, X-ray and Raman lines are reasonably sharp. In addition measurements carried out on a large number of crystals have yielded reproducible results. Further the $x = 0$ powder results of Izumiyama et al. [10] and our $x = 0$, $x \neq 0$ single crystal results match as they both show the presence of specific heat anomaly at T_C where the magnetic transition is far more broader. All these facts are not in favour of the sample inhomogeneity explanation. Similarly the T_c transition (small f_{sc}, H_{c1}, H_{c2}) can in principle be associated with a filamentary minority phase, instead of the BaPrCu2116 phase, assuming the sample to be an impure one. However, by our measurements (EDX, XRD) we have not been able to detect any magnetic or nonmagnetic impurity phase in the crystals. The $x = 0$ sample does not show any superconductivity, so it does not have any filamentary minority superconducting impurity phase (pure system). When Cu is introduced in this $x = 0$ system, no new lines develop in the XRD pattern but the original $x = 0$ sample lines show a shift with x indicating a change in lattice parameters and so incorporation of Cu in the BaPr2116 unit cell rather than its (Cu) precipitation in the lattice as a superconducting minority impurity phase. Raman spectrum too shows this incorporation. The EDX analysis supports 2116 stoichiometry for the system ($x = 0$, $x \neq 0$). Also, the fact that the diamagnetic response is seen in the Fig. 6 inset despite a sizeable positive ($+M$) contribution from SG frozen moments shows that any impurity phase, if responsible for T_c transition, should be present in a quantity detectable by the XRD, EDX measurements. It is actually the resistivity measurements where a filamentary contribution may exist from an undetectable amount of any impurity phase. In addition replacing Pr^{3+} by diamagnetic Y^{3+} in our sample enhances T_c, f_{sc}, H_{c1}, H_{c2} which indicates that the Pr^{3+} spins are responsible for small T_c, f_{sc}, H_{c1}, H_{c2}. Further, as seen in the literature, small T_c, f_{sc}, H_{c1}, H_{c2} generally exist for ruthenocuprates, especially when Cu (carrier) concentration is small, which shows that the Ru spins too are responsible for small T_c, f_{sc}, H_{c1}, H_{c2}. Therefore, in summary, the conclusions drawn in this Letter are acceptable, but the sample microstructure and impurity effects should be kept in mind in any work in this field.

Acknowledgements

This work is supported by the ROC National Science Council grant No. NSC-91-2811-M-007-002PH. Thanks are due to Ms. Nelvi Sutanto for help in crystal growth and Ms. S.R. Huang for the X-ray measurements. One of the authors (S.M.R.) is grateful to the ROC NSC for financial support.

References

[1] Y. Maeno, H. Hashimoto, K. Yoshida, S. Nishizaki, T. Fujita, J.G. Bednorz, F. Lichtenberg, Nature 372 (1994) 532.
[2] D.C. Ling, S.R. Sheen, C.Y. Tai, J.L. Tseng, M.K. Wu, T.Y. Chen, F.Z. Chien, in: B. Batlogg, C.W. Chu, W.K. Chu, D.U. Gubser, K.A. Müller (Eds.), Proceedings of Xth Anniversary HTS Workshop on Physics, Materials and Applications, World Scientific, Singapore, 1996, p. 129.
[3] M.K. Wu, D.Y. Chen, F.Z. Chien, S.R. Sheen, D.C. Ling, C.Y. Tai, G.Y. Tseng, D.H. Chen, F.C. Zhang, Z. Phys. B 102 (1997) 37.
[4] D.Y. Chen, F.Z. Chien, D.C. Ling, J.L. Tseng, S.R. Sheen, M.J. Wang, M.K. Wu, Physica C 282–287 (1997) 73.
[5] C. Bernhard, J.L. Tallon, Ch. Niedermayer, Th. Blasius, A. Golnik, E. Brücher, R.K. Kremer, D.R. Noakes, C.E. Stronach, E.J. Ansaldo, Phys. Rev. B 59 (1999) 14099.
[6] C.A. Cardoso, F.M. Araujo-Moreira, V.P.S. Awana, E. Takayama-Muromachi, O.F. de Lima, H. Yamauchi, M. Karppinen, Phys. Rev. B 67 (2003) 020407(R).
[7] J.W. Lynn, B. Keimer, C. Ulrich, C. Bernhard, J.L. Tallon, Phys. Rev. B 61 (2000) R14964.
[8] R.S. Liu, L.-Y. Jang, H.-H. Hung, J.L. Tallon, Phys. Rev. B 63 (2001) 212507.
[9] K. Kumagai, S. Takada, Y. Furukawa, Phys. Rev. B 63 (2001) 180509(R);
A.C. McLaughlin, J.P. Attfield, Phys. Rev. B 60 (1999) 14605.
[10] Y. Izumiyama, Y. Doi, M. Wakeshima, Y. Hinatsu, Y. Shimojo, Y. Morli, J. Phys.: Condens. Matter 13 (2001) 1303.
[11] Y. Doi, Y. Hinatsu, J. Phys.: Condens. Matter 11 (1999) 4813.
[12] L. Bauernfeind, W. Widder, H.F. Braun, Physica C 254 (1995) 151.

[13] M.T. Anderson, K.B. Greenwood, G.A. Taylor, K.R. Poeppelmeier, Prog. Solid State Chem. 22 (1993) 197.
[14] R. Greatrex, N.N. Greenwood, M. Lal, I. Fernandez, J. Solid State Chem. 30 (1979) 137.
[15] P.D. Battle, W.J. Macklin, J. Solid State Chem. 54 (1984) 245.
[16] P.D. Battle, C.W. Jones, J. Solid State Chem. 78 (1989) 108.
[17] J.K. Srivastava, J. Ferreirinho, S. Ramakrishnan, S.J. Campbell, G. Chandra, R. Vijayaraghavan, Hyperfine Interact. 68 (1991) 279;
J.K. Srivastava, J. Ferreirinho, S. Ramakrishnan, S.J. Campbell, G. Chandra, R. Vijayaraghavan, Hyperfine Interact. 77 (1993) 201, Erratum;
J.K. Srivastava, S. Ramakrishnan, A.K. Nigam, G. Chandra, R. Vijayaraghavan, V. Srinivas, J. Hammann, G. Jéhanno, J.P. Sanchez, Hyperfine Interact. 42 (1988) 1079.
[18] J.K. Srivastava, Phys. Status Solidi (B) 210 (1998) 159;
J.K. Srivastava, in: A. Narlikar (Ed.), Studies of High Temperature Superconductors: Advances in Research and Applications, vol. 29, Nova Science Publishers, Commack, NY, 1999, p. 113;
J.K. Srivastava, in: J.K. Srivastava, S.M. Rao (Eds.), Models and Methods of High-T_c Superconductivity: Some Frontal Aspects, vol. 1, Nova Science Publishers, Hauppauge, NY, 2003, p. 9.
[19] J.K. Srivastava, S. Morimoto, A. Ito, Hyperfine Interact. 54 (1990) 717;
J.K. Srivastava, J. Hammann, K. Asai, K. Katsumata, Phys. Lett. A 149 (1990) 485.
[20] L.E. Wenger, P.H. Keesom, Phys. Rev. B 11 (1975) 3497;
L.E. Wenger, P.H. Keesom, Phys. Rev. B 13 (1976) 4053.
[21] J.C. Ho, D.P. Dandekar, J. Mater. Sci. Lett. 8 (1989) 169;
R.L. Falge Jr., N.M. Wolcott, J. Low Temp. Phys. 5 (1971) 617.
[22] M.A. Señarís-Rodríguez, J.B. Goodenough, J. Solid State Chem. 118 (1995) 323.
[23] Y. Iye, in: A. Narlikar (Ed.), Studies of High Temperature Superconductors: Advances in Research and Applications, vol. 2, Nova Science Publishers, Commack, NY, 1989, p. 210;
G. Marbach, J.W.C. de Vries, M. Klee, H. Passing, S. Stotz, in: A. Narlikar (Ed.), Studies of High Temperature Superconductors: Advances in Research and Applications, vol. 5, Nova Science Publishers, Commack, NY, 1990, p. 171.
[24] E. Gmelin, in: A. Narlikar (Ed.), Studies of High Temperature Superconductors: Advances in Research and Applications, vol. 2, Nova Science Publishers, Commack, NY, 1989, p. 95;
A. Junod, in: D.M. Ginsberg (Ed.), Physical Properties of High Temperature Superconductors II, World Scientific, Singapore, 1990, p. 13.
[25] B.H. Verbeek, J.A. Mydosh, J. Phys. F 8 (1978) L109;
R.N. Kleiman, I. Maartense, G. Williams, Phys. Rev. B 26 (1982) 5241;
J.K. Srivastava, G. Jéhanno, K. Muraleedharan, J.A. Kulkarni, V.R. Marathe, V.S. Darshane, R. Vijayaraghavan, Hyperfine Interact. 28 (1986) 519;
J.K. Srivastava, K. Muraleedharan, R. Vijayaraghavan, Phys. Status Solidi (B) 140 (1987) K47.
[26] J.L. Tallon, J.W. Loram, G.V.M. Williams, C. Bernhard, Phys. Rev. B 61 (2000) R6471;
K. Nakamura, K.T. Park, A.J. Freeman, J.D. Jorgensen, Phys. Rev. B 63 (2000) 024507.